Journal of the American College of Cardiology
© 2008 by the American College of Cardiology Foundation
Published by Elsevier Inc.

Vol. 51, No. 22, 2008
ISSN 0735-1097/08/$34.00
doi:10.1016/j.jacc.2008.01.058

Sirolimus-Induced Vascular Dysfunction

Increased Mitochondrial and Nicotinamide Adenosine Dinucleotide Phosphate Oxidase-Dependent Superoxide Production and Decreased Vascular Nitric Oxide Formation

Alexander Jabs, MD, Sebastian Göbel, MS, Philip Wenzel, MD, Andrei L. Kleschyov, PHD, Marcus Hortmann, MS, Matthias Oelze, PHD, Andreas Daiber, PHD, Thomas Münzel, MD

Mainz, Germany

Objectives This study sought to analyze mechanisms that mediate vascular dysfunction induced by sirolimus.

Background Despite excellent antirestenotic capacity, sirolimus-eluting stents have been found to trigger coronary endothelial dysfunction and impaired re-endothelialization.

Methods To mimic the continuous sirolimus exposure of a stented vessel, Wistar rats underwent drug infusion with an osmotic pump for 7 days.

Results Sirolimus treatment caused a marked degree of endothelial dysfunction as well as a desensitization of the vasculature to the endothelium-independent vasodilator nitroglycerin. Also, sirolimus stimulated intense transmural superoxide formation as detected by dihydroethidine fluorescence in aortae. Increased superoxide production was mediated in part by the vascular nicotinamide adenosine dinucleotide phosphate (NADPH) oxidase as indicated by a marked stimulation of $p67^{phox}$/rac1 NADPH oxidase subunit expression and by increased rac1 membrane association. In addition, superoxide production in rat heart mitochondria was up-regulated by sirolimus, as measured by L012-enhanced chemiluminescence. As a consequence, electron spin resonance measurements showed a 40% reduction in vascular nitric oxide bioavailability, which was further supported by decreased serum nitrite levels.

Conclusions Sirolimus causes marked vascular dysfunction and nitrate resistance after continuous treatment for 7 days. This impaired vasorelaxation may, in part, be induced by up-regulated mitochondrial superoxide release as well as by an up-regulation of NADPH oxidase-driven superoxide production. Both processes could contribute to endothelial dysfunction observed after coronary vascular interventions with sirolimus-coated stents. (J Am Coll Cardiol 2008;51:2130–8) © 2008 by the American College of Cardiology Foundation

Endothelial dysfunction and oxidative stress play an essential role in the progression of atherosclerosis and predict the risk of cardiovascular events in patients with coronary heart disease (CHD) (1). Coronary stent implantation has become a standard treatment modality for patients with symptomatic CHD, and drug-eluting stents (DES) have further improved angiographic and clinical outcomes (2,3). Despite excellent antirestenotic capacity, sirolimus-eluting stents can trigger coronary endothelial dysfunction, impairment of coronary collateral function, late stent thrombosis, and delayed re-endothelialization in some patients (4–9).

Although local drug-related effects are very likely to modulate coronary vascular function, little is known about potential influences of sirolimus on the endothelium. Sirolimus (rapamycin) induces smooth muscle and endothelial cell cycle arrest in the late G1 phase by forming a complex with FK506-binding protein 12 (FKBP12) that inhibits the protein Ser-Thr kinase mammalian target of rapamycin

See page 2139

(mTOR), with mTOR being a central element in signaling pathways involved in the control of cell growth and proliferation (10–12). Recently, Long et al. (13,14) showed that acute in vitro sirolimus treatment as well as genetic deletion of the sirolimus-receptor isoform FKBP12.6 increased protein kinase C (PKC)–mediated endothelial nitric oxide synthase (eNOS) threonine 495 phosphorylation, leading to decreased vascular nitric oxide (NO) production and endothelial dysfunction. However, the effects of a continuous

From the II Medizinische Klinik für Kardiologie und Angiologie, Johannes Gutenberg University, Mainz, Germany. Supported by a vascular biology grant from Cordis GmbH, Langenfeld, Germany (Drs. Jabs and Münzel), a research grant from the Johannes Gutenberg University (Drs. Daiber, Hortmann, and Wenzel), the Deutsche Stiftung für Herzforschung, Frankfurt/M., Germany (Drs. Wenzel and Münzel), and the Deutsche Forschungsgemeinschaft, Bonn, Germany (SFB 553-C17, Drs. Daiber and Münzel).

Manuscript received October 11, 2007; revised manuscript received December 31, 2007, accepted January 21, 2008.

in vivo sirolimus exposure as in a stented vessel (15) on vascular function have not been characterized in detail. Also, the role and sources of oxidative stress in sirolimus-induced vascular dysfunction are not completely understood.

Therefore, in the present study, we established an animal model of vascular dysfunction induced by chronic sirolimus treatment. We found increased reactive oxygen species (ROS) production, and hypothesized that this could contribute to sirolimus-induced vascular dysfunction. We further assessed the transmural distribution of vascular ROS formation, as well as the cellular pathways that could lead to increased superoxide production. Both nicotinamide adenosine dinucleotide phosphate (NADPH) oxidase and mitochondria were found to contribute significantly to the vascular superoxide load after sirolimus treatment.

Methods

Animal Studies

Male Wistar rats (n = 34 in total, 300 to 330 g; Charles River, Sulzfeld, Germany) were anesthetized by isoflurane, and a subcutaneous osmotic minipump (model 1003D, Durect Corp., Cupertino, California) containing either sirolimus (sirolimus group) or the vehicle alone (dimethyl sulfoxide, control group) was implanted. A continuous sirolimus infusion rate of 5 mg/kg/day was used because antiproliferative and immunomodulating effects of sirolimus have been described in the rat neointima model at a dosage between 1.5 and 6 mg/kg/day (16). Systemic levels of sirolimus were measured by high-performance liquid chromatography in whole-blood ethylene diamine tetra-acetic acid samples by the local university clinic core laboratory. Sirolimus concentration in rat blood was 14.2 ± 5.7 μg/l at the time that the animals were euthanized. After 7 days, animals were euthanized under isoflurane anesthesia. Aortae and hearts were carefully removed and processed as described later in the text. All animal investigations conformed to the Guide for the Care and Use of Laboratory Animals as adopted by the U.S. National Institutes of Health. Sirolimus was kindly provided by Wyeth Pharma (Münster, Germany). All other chemicals were purchased from Sigma-Aldrich (St. Louis, Missouri), Merck (Darmstadt, Germany), or Fluka (Buchs, Switzerland).

Vascular Reactivity Studies

Vasodilator responses to the endothelium-dependent vasodilator acetylcholine (ACh) and the endothelium-independent vasodilator nitroglycerin (NTG) were determined in organ chambers by isometric tension studies, as described (17).

Analysis of NO Formation by Spin Trapping as NO-Fe(DETC)$_2$ Complex

Vascular NO formation was detected in rat aortic segments (3 mm) using electron paramagnetic resonance as described (18). Briefly, after an equilibration period, medium was supplemented with 1 μmol/l ACh plus 200 μmol/l colloid Fe(II)-diethyldithiocarbamate (Fe-[DETC]$_2$) and further incubated for 1 h. Vascular rings were then frozen in liquid nitrogen and spectra of electron paramagnetic resonance were recorded at 77 K using an X-band radiospectrometer MS200 (Magnettech, Berlin, Germany). In control experiments, addition of the inhibitor of NO synthase, N^G-nitro-L-arginine methyl ester (L-NAME; 1 mmol/l), completely prevented the formation of NO-Fe(DETC)$_2$ in aortae.

Detection of NO Synthesis as Serum Nitrite

Nitrite, the oxidation product of NO, was analyzed in rat serum by ozone chemiluminescence after chemical reduction to NO as a measure of NO synthesis because nitrite levels correlate with NO biosynthesis (19).

Analysis of Vascular Superoxide Production

Oxidative fluorescent microtopography. The fluorescent dye dihydroethidine (DHE) was used to detect superoxide in situ (20). To assess the influence of eNOS-derived superoxide, vessels were incubated with L-NAME (1 mM) as described (18,20). Also, in some experiments, aortic cross-sections were pre-incubated with the NADPH oxidase inhibitor apocynin (1 mM) (21).

Phorbol myristate (PMA)–induced ROS production. Phorbol myristate–stimulated vascular ROS production was measured using the chemiluminescence indicator reagent Diogenes, a luminol-peroxidase based assay (50% of total reaction volume; National Diagnostics, Atlanta, Georgia) (22). Briefly, aortae were isolated in chilled buffer, cut into 3-mm segments, and incubated for 30 min at 37°C in Hanks buffered salt solution (PAA Laboratories, Pasching, Austria). Then, a mixture of Diogenes containing dimethylsulfoxide (0.1%, vehicle for PMA) and PMA (final concentration 100 nM; Calbiochem, San Diego, California) was added. Chemiluminescence was quantified using a Mithras Microplate Luminometer (Berthold, Bad Wildbad, Germany). Ten-second readings were obtained for each ring over 60 min, and photon counts were normalized for the dry weight of aortic tissue.

Abbreviations and Acronyms

ACh = acetylcholine
CHD = coronary heart disease
DES = drug-eluting stent(s)
DHE = dihydroethidine
eNOS = endothelial nitric oxide synthase
FKBP12 = FK506 binding protein 12
L-NAME = N^G-nitro-L-arginine methyl ester
mPTP = mitochondrial permeability transition pore
mTOR = mammalian target of rapamycin
NADPH = nicotinamide adenosine dinucleotide phosphate
NO = nitric oxide
NOS = nitric oxide synthase
NTG = nitroglycerin
PKC = protein kinase C
PMA = phorbol myristate
qRT-PCR = real-time quantitative reverse-transcriptase polymerase chain reaction
ROS = reactive oxygen species

Real-Time Quantitative Reverse-Transcriptase Polymerase Chain Reaction (qRT-PCR)

The messenger ribonucleic acid (mRNA) expression was analyzed with qRT-PCR as previously described (19). Briefly, total ribonucleic acid from rat aorta was isolated (RNeasy Fibrous Tissue Mini Kit, Qiagen, Hilden, Germany), and 0.5 μg of total ribonucleic acid was used for RT-PCR analysis with the QuantiTect Probe RT-PCR kit (Qiagen). TATA box binding protein (TBP), eNOS, and Nox1 were obtained from MWG-Biotech (Ebersberg, Germany). A TaqMan Gene Expression assay Nox2/gp91^{phox} was purchased as probe-and-primer set (Applied Biosystems, Foster City, California). Sequences of the primers and TaqMan probes were (forward, reverse, and probe) CTTCGTGCCAGAAATGCTGAA, TGTTCGTGGCTCTCTTATTCTCATG, and AATCCCAAGCGGTTTGCTGCAGTCA for TBP; GAGCAGCACAAGAGTTACAAAATCC, TCCACCGCTCGAGCAAAG, and CCACTGGTATCCTCTTGGCGGCG for eNOS; and ACCCCCTGAGTCTTGGAAGTG, GGGTGCATGACAACCTTGGT, and AGGATCCTTCGCTTTTATCGCTCCCG for Nox1. The comparative Ct method was used for relative mRNA quantification; gene expression was normalized to the endogenous control, TBP mRNA; and the amount of target gene mRNA in each sample was expressed relative to that of control.

Detection of Superoxide Formation in Isolated Rat Heart Mitochondria

Mitochondria were prepared from sirolimus-treated and control rats as described (23). Mitochondrial suspensions were diluted to a final protein concentration of 0.1 mg/ml in 0.5 ml of phosphate-buffered saline containing the chemiluminescence dye 8-amino-5-chloro-7-phenylpyridol[3,4-d]pyridozine-1,2-(2H,3H) dione (L012; 100μM), and ROS production was measured after stimulation with succinate (4 mM final concentration) or malate/glutamate (2.5 mM), respectively, as described (23). In a separate series of experiments, mitochondria were treated with cyclosporine A (0.2 μM), glibenclamide (10 μM), diazoxide (100 μM), rotenone (5 μM), antimycin A (20 μg/ml) or myxothiazole (20 μM) before the superoxide measurements (23,24).

Expression and Membrane Association of Protein by Western Blotting

Sample preparation and Western blotting was performed as described (19,25). Incubations were performed with a mouse monoclonal antibody against eNOS (dilution 1:1,000), p67^{phox} (dilution 1:500), rac1 (dilution 1:1000), Nox2 (dilution 1:500) (Transduction Laboratories, Rockford, Illinois), goat polyclonal antibody Nox1 (dilution 1:100; Santa Cruz Biotechnologies, Santa Cruz, California), and rabbit polyclonal p47^{phox} (dilution 1:500, Upstate/Millipore, Billerica, Massachusetts). To determine membrane association of p67^{phox}, p47^{phox}, and rac1, protein homogenates were divided into cytosolic and membrane fractions by ultracentrifugation (1 h, 100,000*g*, 4°C).

Statistical Analysis

Results are expressed as mean ± SEM. The half maximal effective concentration values were obtained by logit transformation. Statistically significant differences were determined using an unpaired 2-sample Student *t* test (SPSS 9.0.1 for Windows, SPSS Inc., Chicago, Illinois). Values of $p < 0.05$ were considered significant.

Results

Effects of Continuous Sirolimus Treatment on Vascular Function and NO Bioavailability

Sirolimus caused endothelial dysfunction as indicated by a markedly reduced vasodilator response of intact rat aortae to the endothelium-dependent vasodilator ACh (Fig. 1A, Table 1). Also, vascular relaxation to the endothelium-independent vasodilator nitroglycerin was impaired (Fig. 1B, Table 1). A significant reduction of NO formation as measured by electron paramagnetic resonance was observed in aortic segments from sirolimus-treated rats (Fig. 1C). Accordingly, serum nitrite was significantly lower in the sirolimus group (Fig. 1D).

Effects of Sirolimus on Vascular ROS Generation

Dihydroethidine staining revealed a strong increase in superoxide throughout all vascular wall layers in aortae from sirolimus-treated animals (Figs. 2A and 2B). Preincubation with the eNOS inhibitor L-NAME specifically increased DHE signaling in the endothelial monolayer of control animals (Fig. 2C), whereas neither transmural DHE fluorescence pattern nor intensity was changed in aorta of sirolimus-treated rats (Fig. 2D). In contrast, incubation of aortic segments with the NADPH oxidase inhibitor apocynin reduced vascular DHE fluorescence in the sirolimus group, albeit not to control levels (Figs. 2E and 2F). Quantitatively, vascular ROS formation in response to activation of protein kinase C with PMA was substantially increased in aortic segments of sirolimus-treated animals (Fig. 3).

Effects of Sirolimus on the Membrane Association of NADPH Oxidase Subunits

Sirolimus up-regulated the expression of the NADPH oxidase subunits p67^{phox} and rac1 in aortic segments (Table 2). Specifically rac1 was found increased in the membrane fraction, that is, in its active membrane-associated form, whereas p67^{phox} and p47^{phox} showed only nonsignificant increases in membrane association (Fig. 4, Table 2). No significant differences were found in the protein expression of the NADPH oxidase isoforms NOX1 and NOX2, although NOX1 mRNA seemed to be up-regulated in sirolimus-treated animals (Table 3). For eNOS, neither

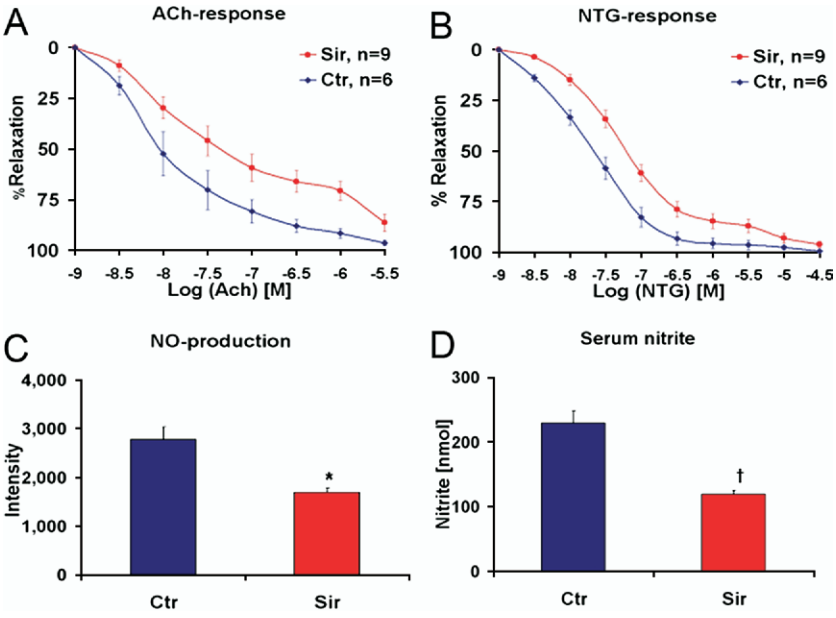

Figure 1 **Effects of Sirolimus on Vascular Function, NO Formation, and Serum Nitrite Levels**

Effects of continuous sirolimus (Sir) infusion (5 mg/kg/day for 7 days) on the concentration response relationship to acetylcholine (ACh) **(A)** and nitroglycerin (NTG) **(B)** in aortic rings. **(C)** Electron paramagnetic resonance showing an approximately 40% reduced vascular nitric oxide (NO) formation after ACh stimulation (*p = 0.001; n = 7 rats per group). **(D)** Decreased serum nitrite levels (−48%; †p = 0.018; n = 5 rats per group). Data are the mean ± SEM of n = 5 **(A, B)**, and 2 **(C, D)** independent experiments. Ctr = control animals.

mRNA nor protein expression showed any changes induced by sirolimus (Table 3).

Effects of Sirolimus on Mitochondrial ROS Formation

Mitochondrial ROS formation was measured using L012-derived chemiluminescence. A significant increase in mitochondrial ROS was observed in the sirolimus group (Fig. 5A). To analyze the underlying intracellular mechanisms contributing to increased mitochondrial ROS formation, we studied the effects of several modulators of mitochondrial function on ROS generation in separate series of experiments: pre-incubation with either cyclosporine A, glibenclamide, or rotenone reduced mitochondrial ROS formation after sirolimus treatment (Fig. 5B). In contrast, incubation with diazoxide did not change ROS generation in mitochondria from sirolimus-treated animals, but triggered a strong increase in the control group to levels similar to those observed in the sirolimus group (Fig. 5B). Also, the respiratory chain inhibitors *Antimycin A* and myxothiazol induced a 15- to 20-fold increase in mitochondrial ROS formation in both control and sirolimus groups (not shown). These findings were consistent for stimulation with the complex II substrate succinate (5 mM) (Fig. 5B) and the complex I substrates malate/glutamate (2.5 mM, not shown).

Table 1 **Effects of Sirolimus on Vascular Reactivity**

In Vivo Treatment	Potency, EC_{50} (−logM)		Efficacy, Maximal Relaxation (%)	
	ACh	NTG	ACh	NTG
Control, n = 6	7.92 ± 0.19	7.66 ± 0.10	96.3 ± 1.4	99.6 ± 0.4
Sirolimus, n = 9	7.44 ± 0.23*	7.22 ± 0.08†	86.4 ± 4.5	96.2 ± 1.6

Vasodilator potency of ACh and NTG in vessels from rats treated with vehicle (DMSO) or sirolimus (5 mg/kg/d) for 7 days. Data are the mean ± SEM of n = 5 independent experiments. *p = 0.034. †p = 0.009.

ACh = acetylcholine; DMSO = dimethyl sulfoxide; EC_{50} = half maximal effective concentration; NTG = nitroglycerin.

Discussion

The results of the present study show that continuous sirolimus treatment causes impaired endothelium-dependent and -independent vascular relaxation, reduced vascular NO bioavailability, and increased vascular ROS formation. This increase is triggered in part by the vascular NADPH oxidase and by increased mitochondrial ROS release. Our findings may provide new insights into the mechanisms that link sirolimus pharmacotherapy to vascular dysfunction, specifically in view of recent clinical data showing impaired coronary endothelial function after sirolimus-eluting stent implantation (4–6).

Sirolimus Induces Vascular Dysfunction

Endothelial-dependent and -independent vasodilator responses were significantly impaired after 7 days of sirolimus treatment (Figs. 1A and 1B, Table 1). Reduced endothelium-dependent vasorelaxation has also been described for short-time in vitro sirolimus incubation of murine aortic rings (13,14); however, reduced vascular

JACC Vol. 51, No. 22, 2008
June 3, 2008:2130–8

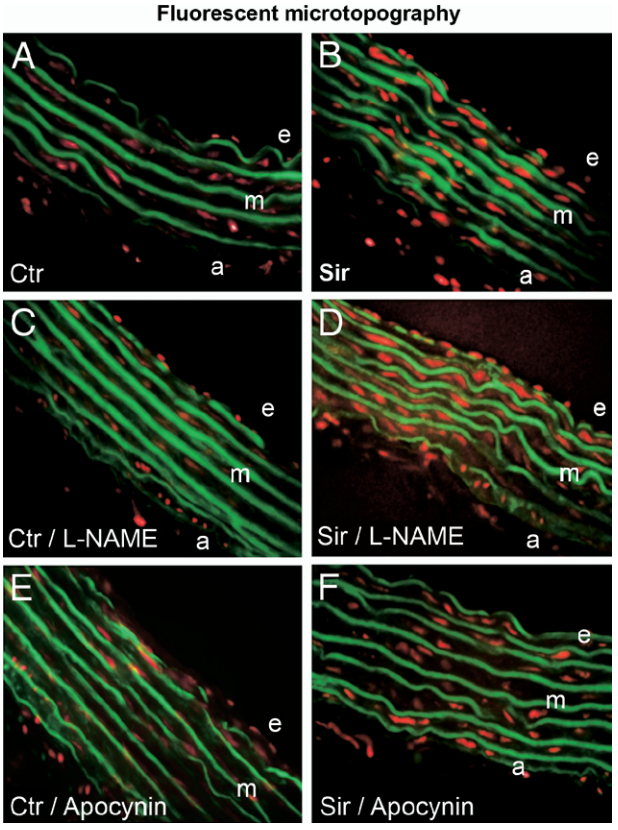

Figure 2 **Effects of Sirolimus on Vascular Superoxide Levels**

Effects of sirolimus (Sir) exposure on vascular superoxide levels as compared to control animals (Ctr). Aortic cross-sections with DHE labeling (1 μM), which produces red fluorescence when oxidized to ethidium by superoxide. Elastic laminae in media (m) with green autofluorescence. Data are representative of n = 3 independent experiments. a = adventitia; DHE = dihydroethidine; e = endothelium; L-NAME = N^G-nitro-L-argine methyl ester.

smooth muscle relaxation to endothelium-independent vasodilators was not observed in these previous studies. Our present findings indicate that sirolimus exposure leads to both endothelial and smooth muscle cell dysfunction. Because steady state arterial tissue concentrations are approached only after several days of drug exposure (26), a continuous sirolimus treatment as used in the current study seems essential to assess drug effects in the media. Also, a significant −40% reduction in vascular NO bioavailability was observed in the sirolimus group (Fig. 1C). Reduced NO formation also has been shown after acute in vitro sirolimus exposure of vascular homogenates (13), whereas a slight increase of NO content was reported in human microvascular endothelial cells (27). However, the marked decrease in serum nitrite (Fig. 1D), the oxidation product of NO whose concentration correlates with NO biosynthesis (19,28), further supports our finding of reduced NO availability after sirolimus treatment. Likewise, sirolimus has been shown to induce oxidative stress in cultured human microvascular endothelial cells (27), whereas in another in vitro study, no effect of sirolimus on superoxide production was observed in human umbilical vein endothelial cells (29).

Sirolimus Causes Increased Vascular ROS Formation

Because vascular NO is metabolized by the superoxide anion, we hypothesized that continuous sirolimus exposure may stimulate vascular superoxide production. Indeed, we detected a strong increase in superoxide levels that was not restricted to the endothelium cell layer but was observed throughout the vascular wall (Figs. 2A and 2B). To check for an involvement of the vascular NADPH oxidase, which is activated by protein kinase C (PKC), vessels were exposed to the direct PKC activator PMA. Indeed, phorbol ester-induced vascular ROS formation was found significantly up-regulated in the sirolimus group (Fig. 3).

Sirolimus Activates NADPH Oxidase-Dependent ROS Production

To further assess the involvement of the NADPH oxidase, aortic cross-sections were pre-incubated with the NADPH oxidase inhibitor apocynin (Figs. 2E and 2F), which was indeed able to drastically reduce vascular superoxide production. Cytosolic NADPH oxidase subunits $p67^{phox}$ and rac1 were significantly up-regulated in sirolimus-treated aortae; a trend toward increased expression was also seen for $p47^{phox}$ (Table 2). The rac1 protein was found specifically increased in the membrane fraction, that is, in its active form (Fig. 4). Because the small GTP-binding protein rac1 is known to be activated during endothelial NADPH oxidase activation (30), our present findings are compatible with increased NADPH oxidase activity in response to sirolimus treatment (Fig. 4). Up-regulation of rac1 among other NADPH oxidase subunits has also been described for

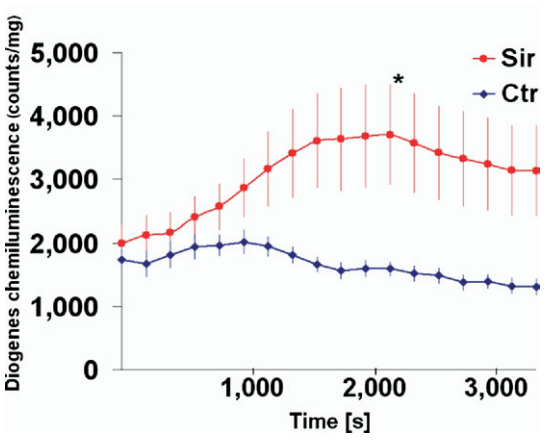

Figure 3 **Effects of Sirolimus on Phorbol Ester-Induced Vascular ROS Formation**

Time course of phorbol myristate-stimulated ROS production in aortic rings measured by a luminol-peroxidase based assay. *p = 0.021; n = 3 animals per group. Ctr = control animals; ROS = reactive oxygen species; Sir = sirolimus.

Table 2 Effects of Sirolimus on the Expression of NADPH Oxidase Subunits

In Vivo Treatment	$p67^{phox}$			$p47^{phox}$			rac1		
	Hg	Cyt	Mem	Hg	Cyt	Mem	Hg	Cyt	Mem
Control	1.00 ± 0.14	0.74 ± 0.15	0.26 ± 0.04	1.00 ± 0.07	0.42 ± 0.04	0.58 ± 0.06	1.00 ± 0.07	0.30 ± 0.04	0.70 ± 0.06
Sirolimus	1.59 ± 0.21*	1.15 ± 0.15	0.45 ± 0.08	1.13 ± 0.13	0.42 ± 0.06	0.71 ± 0.09	1.65 ± 0.07†	0.69 ± 0.07†	0.96 ± 0.03‡

Effects of sirolimus treatment on expression and membrane association of the soluble NADPH oxidase subunits $p67^{phox}$, $p47^{phox}$, and rac1. Data are the mean ± SEM, n = 5 to 7 animals per group. *p = 0.039. †p < 0.001. ‡p = 0.005.

Cyt = cytosolic fraction; Hg = total protein homogenate; Mem = membrane fraction; NADPH = nicotinamide adenosine dinucleotide phosphate.

the FKBP12 binding immunosuppressant FK506 in a rat renal transplant model (31). No significant changes were found for NOX1 and NOX2 protein expression, indicating that increased NADPH oxidase mediated ROS formation after sirolimus treatment is caused by stimulation of cytosolic NADPH oxidase subunit expression and by rac1 membrane translocation (Fig. 6) (32). Previously, we have shown that increased NADPH oxidase-mediated superoxide production may act as a kindling radical leading to eNOS uncoupling, for example, in diabetes (20) and in angiotensin II hypertension (33).

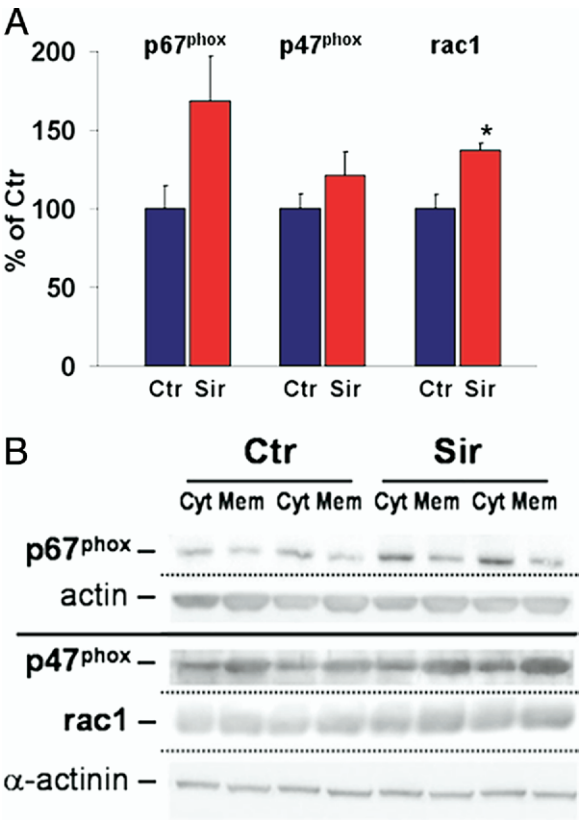

Figure 4 Effects of Sirolimus on Membrane Association of Soluble NADPH Oxidase Subunits

Effects of sirolimus on membrane association of the soluble NADPH oxidase subunits $p67^{phox}$, $p47^{phox}$, and rac1. **(A)** Immunoblotting analysis of indicated subunits in the membrane fraction with densimetric quantification and **(B)** original blots. *p = 0.005 versus Ctr; n = 5 to 7 animals per group. Cyt = cystolic fraction; Mem = membrane fraction; NADPH = nicotinamide adenosine dinucleotide phosphate; other abbreviations as in Figure 3.

Sirolimus Does Not Induce eNOS Uncoupling

The DHE-stained vessels were incubated with the eNOS inhibitor L-NAME. N^G-nitro-L-arginine methyl ester did not induce any changes in DHE signaling in the sirolimus group, whereas endothelial superoxide increased in control subjects (Figs. 2C and 2D). Hence, eNOS-derived NO quenches basal levels of superoxide in control animals, whereas uncoupled eNOS seems not to be a significant source of superoxide after sirolimus treatment. In addition, eNOS mRNA and protein expression was not changed by sirolimus (Table 3), as also observed for acute sirolimus treatment (13). Importantly, DHE fluorescence was not reduced to control levels by the NADPH oxidase inhibitor apocynin (Fig. 2F), pointing to other ROS sources being activated in response to sirolimus treatment.

Mitochondrial ROS Contribute to Sirolimus-Induced Oxidative Stress

The mitochondrial respiratory chain is the major source of ROS in most mammalian cells, and excess production of mitochondrial ROS has been implicated in aging and cardiovascular diseases such as atherosclerosis, hypertension, and diabetes (34,35). A pronounced increase in mitochondrial ROS was induced by continuous sirolimus treatment (Fig. 5A), whereas short-term in vitro incubation of isolated mitochondria with sirolimus had no effect on superoxide production (not shown). This effect was partially reversed by mitochondrial pre-incubation with the mitochondrial permeability transition pore (mPTP) blocker cyclosporine A, the K_{ATP} channel inhibitor glibenclamide, and the complex I inhibitor rotenone (Figs. 5B and 6). Treatment with the K_{ATP} channel opener diazoxide did not change sirolimus-induced mitochondrial ROS formation, but triggered mitochondrial ROS in the control group (Fig. 5B). These findings indicate that sirolimus treatment could lead to K_{ATP} channel opening by increasing intracellular superoxide, whereas direct effects of sirolimus on mitochondrial ion channels are not supported by our present data. The mitochondrial respiratory chain complexes I to III have been identified as major sites of ROS production in human umbilical vein endothelial cells and human coronary arteriolar endothelial cells (36,37). Opening of mPTP is known to induce the efflux of superoxide from

Table 3 Effects of Sirolimus on the Expression of NOX1, NOX2, and eNOS

	Relative mRNA Expression			Relative Protein Expression		
In Vivo Treatment	NOX1	NOX2	eNOS	NOX1	NOX2	eNOS
Control	1.00 ± 0.07	1.00 ± 0.13	1.00 ± 0.07	1.00 ± 0.12	1.00 ± 0.59	1.00 ± 0.29
Sirolimus	3.11 ± 0.53*	0.97 ± 0.53	1.13 ± 0.08	0.89 ± 0.10	0.89 ± 0.34	0.86 ± 0.14

Sirolimus treatment has no significant effects on indicated mRNA (except NOX1) and protein expression in rat aorta as determined by real-time polymerase chain reaction and Western blotting, respectively. Data are the mean ± SEM, n = 5 to 7 animals per group. *p = 0.003.
eNOS = endothelial nitric oxide synthase; mRNA = messenger ribonucleic acid; NOX = nicotinamide adenosine dinucleotide phosphate oxidase.

the mitochondrial matrix into the cytoplasm, an effect that can be triggered by the opening of K_{ATP} channels, which itself can be induced by cytosolic ROS (38). Therefore, it is tempting to speculate that sirolimus-induced increases in cytosolic ROS from NADPH oxidases may contribute to the opening of K_{ATP} channels and subsequent ROS release from mitochondria via the mPTP (Fig. 6).

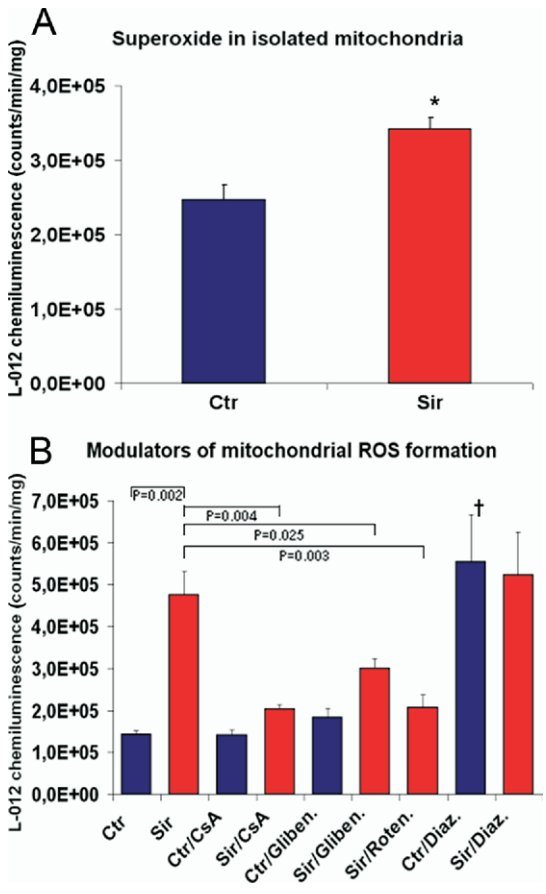

Figure 5 Effects of Sirolimus on Mitochondrial ROS Formation

Mitochondrial ROS formation after in vivo sirolimus treatment for 7 days. **(A)** Increased formation of ROS in response to sirolimus as detected using L012-derived chemiluminescence in isolated mitochondria. *p = 0.020; n = 8 animals control, n = 10 animals sirolimus. **(B)** Modulation of mitochondrial ROS formation by cyclosporine A (CsA, 0.2 μM), glibenclamide (Gliben., 10 μM), rotenone (Roten., 5 μM), and diazoxide (Diaz., 100 μM). †p = 0.005 for Ctr versus Ctr/Diaz., other p values as indicated. n = 5 animals per group. Abbreviations as in Figure 3.

Study Limitations

The current study can only provide limited insight into the pathophysiological mechanisms leading to impaired coronary endothelial function in a clinical setting after stent implantation (4–6), given limitations such as the comparability of rodent and human vasoreactivity, divergent vasodilator responses in different vascular beds, absence of pre-existing atherosclerotic plaques, and lack of the specific drug-release kinetics provided by sirolimus-eluting stents (15). Also, it seems conceivable that oral medication in CHD patients could interfere with sirolimus-induced vascular ROS production (19,39,40) whereas coronary inflammatory cell chemotaxis may further increase local oxidative stress after angioplasty (41,42). Given the species-specific elimination and degradation half-life of sirolimus (43), comparisons of drug concentrations among different species must be interpreted cautiously. Also, none of the previous clinical studies could conclusively explain the phenomenon of endothelial dysfunction at 6 months (4,5), whereas drug release is almost completed within 30 days. Herein, either the high tissue binding capacity and prolonged elution of sirolimus (26) and/or the persistent presence of the stent polymer (44) may contribute to endothelial dysfunction and impaired re-endothelialization. However, recent clinical data identify endothelial dysfunction as early as 2 weeks after sirolimus-eluting stent implantation (6). In addition, possible vascular side effects or adaptive mechanisms of a continuous systemic sirolimus treatment, as in organ transplant patients, cannot be extrapolated from the current data. However, our findings clearly show sirolimus-induced vascular dysfunction and identify intracellular signaling pathways that contribute to reduced vascular NO availability and increased ROS formation, and thereby clearly point to mechanisms leading to vascular side effects of sirolimus.

Summary and Clinical Implications

Continuous sirolimus exposure causes impaired endothelium-dependent and -independent vascular relaxation, reduced vascular NO formation, and increased transmural ROS production. This increase is triggered by NADPH oxi-

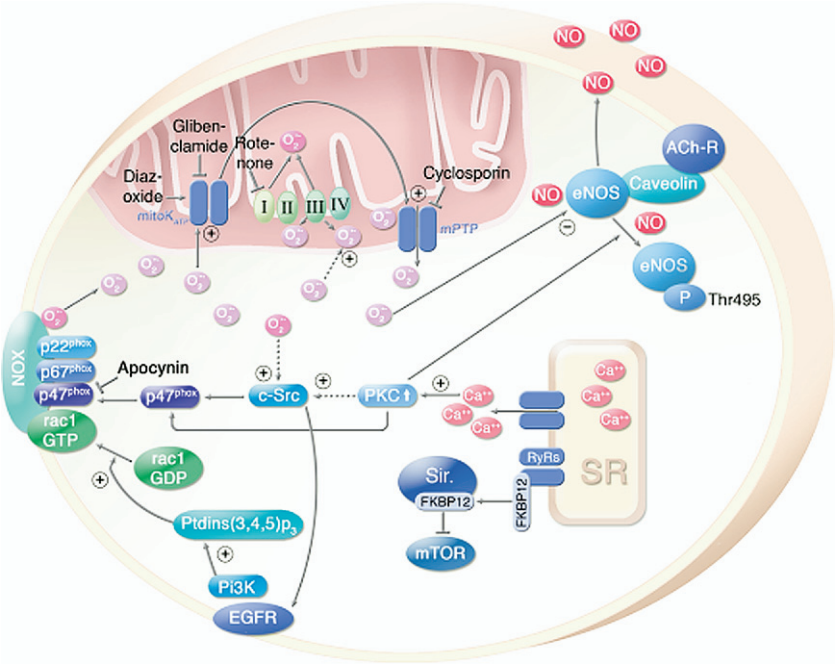

Figure 6 **Proposed Scheme of the Mechanisms Underlying Sirolimus-Induced Vascular Dysfunction**

Sirolimus (Sir) forms a complex with its receptor FK506-binding protein 12 (FKBP12), leading to cell cycle arrest by inhibition of mammalian target of sirolimus (mTOR) (10–12). Removal of FKBP12 from ryanodine receptors (RyRs) induces efflux of calcium (Ca^{2+}) from the sarcoplasmic reticulum (SR), leading to protein kinase C (PKC)–mediated eNOS-Thr495 phosphorylation and consecutive reduction in NO production (14). Increased PKC activity can also induce NADPH oxidase mediated superoxide (O_2^-) production, in part by induction of rac1 membrane association (reviewed by Cai et al. [32]). Intracellular O_2^- reacts with and stimulates ATP-sensitive K^+ channels ($mitoK_{ATP}$) in the inner mitochondrial membrane, leading to opening of the mitochondrial permeability transition pore (mPTP) and consecutive efflux of large amounts of O_2^- into the cytoplasm. This concept of ROS-triggered ROS formation has first been described in ischemic and angiotensin II-induced pre-conditioning [as reviewed by Brandes (38)]. The main source of mitochondrial ROS is the respiratory chain, indicated by complexes I to IV. Inhibition of K_{APT} channel opening as well as mPTP opening significantly decreased sirolimus-induced ROS formation. Sirolimus-induced ROS can further decrease NO bioavailability, leading to vascular dysfunction. ACh-R = acetylcholine receptor; ATP = adenosine triphosphate; c-Src = cellular homologue of the transforming gene of Rous sarcoma virus; EGFR = epidermal growth factor receptor; eNOS = endothelial nitric oxide synthase; GDP = guanosine diphosphate; GTP = guanosine triphosphate; NADPH = nicotinamide adenosine dinucleotide phosphate; NO = nitric oxide; p = phosphate-residue; Pi3K = phosphatidylinositol 3-kinase; Ptd(3,4,5)P3 = phosphatidylinositol (3,4,5)-trisphosphate; ROS = reactive oxygen species.

dase expression and membrane association as well as stimulation of mitochondrial ROS release. These drug effects could very well contribute to clinically observed vascular dysfunction after sirolimus-eluting stent implantation, and their specific antagonization could help to optimize efficacy and safety of future pharmacological antirestenotic approaches.

Acknowledgments

The authors thank Jörg A. Schreiner for expert technical assistance. This article contains results that are part of the thesis work of Sebastian Göbel.

Reprint requests and correspondence: Dr. Thomas Münzel, II Medizinische Klinik und Poliklinik, Johannes Gutenberg Universität Mainz, Langenbeckstrasse 1, 55131 Mainz, Germany. E-mail: tmuenzel@uni-mainz.de.

REFERENCES

1. Heitzer T, Schlinzig T, Krohn K, et al. Endothelial dysfunction, oxidative stress, and risk of cardiovascular events in patients with coronary artery disease. Circulation 2001;104:2673–8.
2. Williams DO, Abbott JD, Kip KE. Outcomes of 6906 patients undergoing percutaneous coronary intervention in the era of drug-eluting stents: report of the DEScover Registry. Circulation 2006;114:2154–62.
3. Zahn R, Hamm CW, Schneider S, et al. The sirolimus-eluting coronary stent in daily routine practice in Germany. Clin Res Cardiol 2007;96:548–56.
4. Togni M, Windecker S, Cocchia R, et al. Sirolimus-eluting stents associated with paradoxic coronary vasoconstriction. J Am Coll Cardiol 2005;46:231–6.
5. Hofma SH, van der Giessen WJ, van Dalen BM, et al. Indication of long-term endothelial dysfunction after sirolimus-eluting stent implantation. Eur Heart J 2006;27:166–70.
6. Obata J, Kitta Y, Takano H, et al. Sirolimus-eluting stent implantation aggravates endothelial vasomotor dysfunction in the infarct-related coronary artery in patients with acute myocardial infarction. J Am Coll Cardiol 2007;50:1305–9.
7. Meier P, Zbinden R, Togni M, et al. Coronary collateral function long after drug-eluting stent implantation. J Am Coll Cardiol 2007;49:15–20.
8. Jensen LO, Maeng M, Kaltoft A, et al. Stent thrombosis, myocardial infarction, and death after drug-eluting and bare-metal stent coronary interventions. J Am Coll Cardiol 2007;50:463–70.
9. Luscher TF, Steffel J, Eberli FR, et al. Drug-eluting stent and coronary thrombosis: biological mechanisms and clinical implications. Circulation 2007;115:1051–8.
10. Poon M, Marx SO, Gallo R, et al. Rapamycin inhibits vascular smooth muscle cell migration. J Clin Invest 1996;98:2277–83.

11. Guba M, von Breitenbuch P, Steinbauer M, et al. Rapamycin inhibits primary and metastatic tumor growth by antiangiogenesis: involvement of vascular endothelial growth factor. Nat Med 2002;8:128–35.
12. Harris TE, Lawrence JC Jr. TOR signaling. Sci STKE 2003;212:re15.
13. Long C, Cook LG, Wu GY, Mitchell BM. Removal of FKBP12/12.6 from endothelial ryanodine receptors leads to an intracellular calcium leak and endothelial dysfunction. Arterioscler Thromb Vasc Biol 2007;27:1580–6.
14. Long C, Cook LG, Hamilton SL, et al. FK506 binding protein 12/12.6 depletion increases endothelial nitric oxide synthase threonine 495 phosphorylation and blood pressure. Hypertension 2007;49:569–76.
15. Yang C, Burt HM. Drug-eluting stents: factors governing local pharmacokinetics. Adv Drug Deliv Rev 2006;58:402–11.
16. Gregory CR, Huie P, Billingham ME, Morris RE. Rapamycin inhibits arterial intimal thickening caused by both alloimmune and mechanical injury. Its effect on cellular, growth factor, and cytokine response in injured vessels. Transplantation 1993;55:1409–18.
17. Munzel T, Sayegh H, Freeman BA, et al. Evidence for enhanced vascular superoxide anion production in nitrate tolerance. A novel mechanism underlying tolerance and cross-tolerance. J Clin Invest 1995;95:187–94.
18. Kleschyov AL, Munzel T. Advanced spin trapping of vascular nitric oxide using colloid iron diethyldithiocarbamate. Methods Enzymol 2002;359:42–51.
19. Oelze M, Daiber A, Brandes RP, et al. Nebivolol inhibits superoxide formation by NADPH oxidase and endothelial dysfunction in angiotensin II-treated rats. Hypertension 2006;48:677–84.
20. Hink U, Li H, Mollnau H, et al. Mechanisms underlying endothelial dysfunction in diabetes mellitus. Circ Res 2001;88:E14–22.
21. Oelze M, Warnholtz A, Faulhaber J, et al. NADPH oxidase accounts for enhanced superoxide production and impaired endothelium-dependent smooth muscle relaxation in BKbeta1−/− mice. Arterioscler Thromb Vasc Biol 2006;26:1753–9.
22. Lavigne MC, Malech HL, Holland SM, Leto TL. Genetic demonstration of p47phox-dependent superoxide anion production in murine vascular smooth muscle cells. Circulation 2001;104:79–84.
23. Daiber A, Oelze M, August M, et al. Detection of superoxide and peroxynitrite in model systems and mitochondria by the luminol analogue L-012. Free Radic Res 2004;38:259–69.
24. Wenzel P, Mollnau H, Oelze M, et al. First evidence for crosstalk between mitochondrial and NADPH oxidase-derived reactive oxygen species in nitroglycerin-triggered vascular dysfunction. Antioxid Redox Signal 2008. In press.
25. Mollnau H, Oelze M, August M, et al. Mechanisms of increased vascular superoxide production in an experimental model of idiopathic dilated cardiomyopathy. Arterioscler Thromb Vasc Biol 2005;25:2554–9.
26. Levin AD, Vukmirovic N, Hwang CW, Edelman ER. Specific binding to intracellular proteins determines arterial transport properties for rapamycin and paclitaxel. Proc Natl Acad Sci U S A 2004;101:9463–7.
27. Trapp A, Weis M. The impact of immunosuppression on endothelial function. J Cardiovasc Pharmacol 2005;45:81–7.
28. Lauer T, Preik M, Rassaf T, et al. Plasma nitrite rather than nitrate reflects regional endothelial nitric oxide synthase activity but lacks intrinsic vasodilator action. Proc Natl Acad Sci U S A 2001;98:12814–9.
29. Krotz F, Keller M, Derflinger S, et al. Mycophenolate acid inhibits endothelial NAD(P)H oxidase activity and superoxide formation by a Rac1-dependent mechanism. Hypertension 2007;49:201–8.
30. Krotz F, Engelbrecht B, Buerkle MA, et al. The tyrosine phosphatase, SHP-1, is a negative regulator of endothelial superoxide formation. J Am Coll Cardiol 2005;45:1700–6.
31. Khanna AK, Pieper GM. NADPH oxidase subunits (NOX-1, p22phox, Rac-1) and tacrolimus-induced nephrotoxicity in a rat renal transplant model. Nephrol Dial Transplant 2007;22:376–85.
32. Cai H, Griendling KK, Harrison DG. The vascular NAD(P)H oxidases as therapeutic targets in cardiovascular diseases. Trends Pharmacol Sci 2003;24:471–8.
33. Mollnau H, Wendt M, Szocs K, et al. Effects of angiotensin II infusion on the expression and function of NAD(P)H oxidase and components of nitric oxide/cGMP signaling. Circ Res 2002;90:E58–65.
34. Zhang DX, Gutterman DD. Mitochondrial reactive oxygen species-mediated signaling in endothelial cells. Am J Physiol Heart Circ Physiol 2007;292:H2023–31.
35. Warnholtz A, Wendt M, Munzel T. When sleeping beauty turns ugly: mitochondria in hypoxia. Arterioscler Thromb Vasc Biol 2002;22:525–7.
36. Therade-Matharan S, Laemmel E, Carpentier S, et al. Reactive oxygen species production by mitochondria in endothelial cells exposed to reoxygenation after hypoxia and glucose depletion is mediated by ceramide. Am J Physiol Regul Integr Comp Physiol 2005;289:R1756–62.
37. Liu Y, Zhao H, Li H, et al. Mitochondrial sources of H2O2 generation play a key role in flow-mediated dilation in human coronary resistance arteries. Circ Res 2003;93:573–80.
38. Brandes RP. Triggering mitochondrial radical release: a new function for NADPH oxidases. Hypertension 2005;45:847–8.
39. Wassmann S, Laufs U, Muller K, et al. Cellular antioxidant effects of atorvastatin in vitro and in vivo. Arterioscler Thromb Vasc Biol 2002;22:300–5.
40. Warnholtz A, Nickenig G, Schulz E, et al. Increased NADH-oxidase-mediated superoxide production in the early stages of atherosclerosis: evidence for involvement of the renin-angiotensin system. Circulation 1999;99:2027–33.
41. Bauriedel G, Jabs A, Skowasch D, et al. Dendritic cells in neointima formation after rat carotid balloon injury: coordinated expression with anti-apoptotic Bcl-2 and HSP47 in arterial repair. J Am Coll Cardiol 2003;42:930–8.
42. Jabs A, Okamoto E, Vinten-Johansen J, et al. Sequential patterns of chemokine- and chemokine receptor-synthesis following vessel wall injury in porcine coronary arteries. Atherosclerosis 2007;192:75–84.
43. Ferron GM, Jusko WJ. Species differences in sirolimus stability in humans, rabbits, and rats. Drug Metab Dispos 1998;26:83–4.
44. Udipi K, Chen M, Cheng P, et al. Development of a novel biocompatible polymer system for extended drug release in a next-generation drug-eluting stent. J Biomed Mater Res A 2008;85:1064–71.